



Centrum voor Wiskunde en Informatica

**REPORT***RAPPORT*

**MAS**

*Modelling, Analysis and Simulation*



*Modelling, Analysis and Simulation*

Adaptive grid simulations of negative streamers in  
nitrogen in under- and overvolted gaps

C. Montijn, U. Ebert, W. Hundsdorfer

**REPORT MAS-E0528 DECEMBER 2005**

CWI is the National Research Institute for Mathematics and Computer Science. It is sponsored by the Netherlands Organization for Scientific Research (NWO).

CWI is a founding member of ERCIM, the European Research Consortium for Informatics and Mathematics.

CWI's research has a theme-oriented structure and is grouped into four clusters. Listed below are the names of the clusters and in parentheses their acronyms.

Probability, Networks and Algorithms (PNA)

Software Engineering (SEN)

**Modelling, Analysis and Simulation (MAS)**

Information Systems (INS)

Copyright © 2005, Stichting Centrum voor Wiskunde en Informatica

P.O. Box 94079, 1090 GB Amsterdam (NL)

Kruislaan 413, 1098 SJ Amsterdam (NL)

Telephone +31 20 592 9333

Telefax +31 20 592 4199

ISSN 1386-3703

# Adaptive grid simulations of negative streamers in nitrogen in under- and overvolted gaps

## ABSTRACT

A local uniform grid refinement strategy is implemented for the simulation of negative anode-directed streamers. The results are shown for an undervolted gap filled with nitrogen at 300 K, with a uniform background electric field of 30 kV/cm. The build up of space charge during the electron avalanche is sped up by a net inflow of electrons at the cathode. The streamer then propagates in the self-induced field enhancement of the space charge layer. Eventually, the streamer branches. The results are compared to those in an overvolted gap (background field of 100 kV/cm). In this case the propagation has the same qualitative features as in the undervolted gap, but the streamer velocity is a factor four larger, while the time to branching is sped up with roughly a factor hundred.

*2000 Mathematics Subject Classification:* 35K57 ; 65M50 ; 78A35

*Keywords and Phrases:* Electric breakdown; adaptive grid refinements;

*Note:* This work was financially supported by the Netherlands Organisation for Scientific Research NWO within the Computational Science programme. The paper appeared in the refereed proceedings of the XXVII'th Int. Conf. on Phenomena in Ionized Gases (ICPIG), Veldhoven 2005.



# Adaptive grid simulations of negative streamers in nitrogen in under- and overvolted gaps

C. Montijn<sup>1</sup>, U. Ebert<sup>1,2</sup>, W. Hundsdorfer<sup>1</sup>

<sup>1</sup> Centrum voor Wiskunde en Informatica, P.O.Box 94079, 1090 GB Amsterdam, the Netherlands

<sup>2</sup> Eindhoven University of Technology, P.O. Box 513, 5600 MB Eindhoven, the Netherlands

*A local uniform grid refinement strategy is implemented for the simulation of negative anode-directed streamers. The results are shown for an undervolted gap filled with nitrogen at 300 K, with a uniform background electric field of 30 kV/cm. The build up of space charge during the electron avalanche is sped up by a net inflow of electrons at the cathode. The streamer then propagates in the self-induced field enhancement of the space charge layer. Eventually, the streamer branches. The results are compared to those in an overvolted gap (background field of 100 kV/cm). In this case the propagation has the same qualitative features as in the undervolted gap, but the streamer velocity is a factor four larger, while the time to branching is sped up with roughly a factor hundred.*

## 1 Introduction

When a sufficiently strong electric field is applied to a gas, electron avalanches eventually build up a region with high space charge and turn into discharge streamers. These are highly ionized, non-equilibrium plasma channels, with a tip surrounded by a thin space charge layer. The rapid growth of the streamers is a result of the self-induced field enhancement at the tip due to this curved layer.

The high reactivity of the radicals they emit make them suitable for a wide variety of industrial applications [1, 2]. They can also be observed in nature, where new techniques showed the existence of sprites and blue jets in the higher regions of the atmosphere [3].

While in many applications the streamers propagate in a non-uniform field into a complex mixture of gas, we here focus on the basic phenomenon of primary anode directed streamers in a non-attaching and non-ionized gas like nitrogen, with a uniform background electric field.

## 2 The minimal streamer model

The essential properties of the negative streamer propagation in a non-attaching gas can be analyzed by the minimal streamer model for two species of charged particles (electrons and positive ions). This is a fluid approximation for the particles, which includes drift in the electric field  $\mathbf{E}$ , diffusion, and a local field-dependent impact ionization term  $S_i$ .

$$\partial_t n_e = \nabla \cdot (n_e \mu_e \mathbf{E}) + D_e \nabla^2 n_e + S_i, \quad (1)$$

$$\partial_t n_+ = S_i. \quad (2)$$

Here  $n_e$  and  $n_+$  are the electron and positive ion densities,  $D_e$  is the electron diffusion coefficient. The ions can be considered to be immobile on the short time scales considered here, since their mobility is two orders of magnitude smaller than that of the electrons. The reaction term is given by Townsend's approximation for the impact ionization,

$$S_i = n_e \mu_e |\mathbf{E}| \alpha(|\mathbf{E}|) = n_e \mu_e |\mathbf{E}| \alpha_0 e^{-E_T/|\mathbf{E}|}, \quad (3)$$

in which  $\alpha_0$  is the ionization coefficient. The electric field  $\mathbf{E}$  is determined through Poisson's equation for the electric potential,

$$\nabla^2 \phi = \frac{e}{\epsilon_0} (n_e - n_+), \quad \mathbf{E} = -\nabla \phi, \quad (4)$$

where  $e$  is the elementary charge.

This model has been implemented in dimensionless form. The dimensionless quantities have been defined through scaling with the natural scales of length  $l_0$ , time  $t_0$ , field  $E_T$ , charge density  $n_0$  and diffusion  $D_0$ .  $l_0$  and  $E_T$  come from Townsend's ionization formula,  $l_0$  corresponding to the inverse of the ionization coefficient and  $E_T$  being the characteristic impact ionization field.  $l_0$  and  $E_T$  are known to be inversely proportional and proportional to the pressure  $p$ , respectively [4]. The characteristic velocity then becomes  $v_0 = \mu_e E_T$ , leading to a characteristic timescale  $t_0 = l_0/v_0$ . Because the electron mobility scales with the inverse of the pressure, so will the characteristic time scale. The natural scale of charge density emerges from the Poisson equation,  $n_0 = \epsilon_0 E_T / e l_0$ . The scaling factor for the diffusion coefficient comes from the continuity equations,  $D_0 = l_0^2 / t_0$ . With  $\mu_e$ ,  $l_0$  and  $E_T$  from [5, 6]

for nitrogen at 300K, we have, as a function of the pressure  $p$  in bar:

$$\begin{aligned}\mu_e &\simeq 380\text{cm}^2\text{V}^{-1}\text{s}^{-1}/p, & t_0 &\simeq 3\text{ps}/p, \\ l_0 &\simeq 2.3\text{ }\mu\text{m}/p, & n_0 &\simeq 4.7 \cdot 10^{14}/\text{ecm}^{-3}p^2, \\ E_T &\simeq 200\text{kVcm}^{-1}p, & D_0 &\simeq 1.8 \cdot 10^4\text{cm}^2\text{s}^{-1}/p.\end{aligned}$$

For the sake of legibility the results will be presented in dimensional units corresponding to  $\text{N}_2$  at 300 K and at atmospheric pressure. It should be kept in mind that rescaling makes it possible to convert the results to other pressures, (pure, non-attaching) gas types, etc.

### 3 Numerical method

We consider two plane-parallel electrodes in a radially symmetric system  $(r, z)$ . The cathode is situated at  $z = 0$ , the anode at  $L_z$ . An initial Gaussian ionization seed on the axis of symmetry is subjected to the background field  $\mathbf{E}_0 = -E_0\hat{e}_z$  and propagates towards the anode. The initial seed is characterized by the maximum value  $\sigma_0$ , its position  $z_0$  on the axis, and the  $1/e$  radius  $r_e$ . The boundary conditions for the particle densities are homogeneous Neumann at the anode as well as at the radial boundary. At the cathode, the choice can be made between homogeneous Neumann and Dirichlet boundary conditions. The first means a net electron flux may enter the system, while the latter corresponds to a no-flow condition. The potential is imposed on the electrodes, and a homogeneous Neumann boundary condition is set at the  $r$ -boundary.

Eventually, a thin space charge layer appears at the tip of the streamer, requiring a high spatial accuracy of the discretizations. In order to achieve this within the limitations of computational memory and time, the model is implemented using local uniform grid refinements.

An explicit method (two-stage Runge-Kutta) is used for the time stepping, making it possible to decouple the grids for the continuity equations (1)-(2) from those for the Poisson equation (4). In both cases, a series of time-dependent, uniformly refined, nested grids is used.

The refinement criterion for the particle grids is based on the curvatures of the electron and net charge density distributions, that give an estimate of the spatial error in the solution on a certain grid [7]. The spatial discretization is based on finite volumes. The drift term is computed using a third order flux limiting scheme with Koren limiter.

This scheme prevents the appearance of spurious oscillations in the solution, that may appear with a third order upwind-biased scheme, by switching to a first order scheme in regions with large spatial gradients [8]. The diffusion term is computed with a second order central discretization. A charge conserving, piecewise bilinear interpolation is used to map coarse grid values to fine grids. Charge conservation is ensured at the grid interfaces with a flux correction.

The refinement criterion for the potential grids is based on the difference between the solutions on two consecutive grids. On each grid, the Poisson equation is solved using FISHPACK, a fast Poisson solver using a second-order central discretization and based on a cyclic reduction method. The boundary conditions for fine grids are computed with a third-order quadratic interpolation of the coarse grid values. The source term, i.e. the net charge density distribution, is mapped to coarser potential grids through mass conserving restrictions, and to finer grids using a third order interpolation. The electric field is computed with a second order discretization of Eq.(4) on each potential grid. If a particle grid is finer than the finest potential grid, the field is computed through a piecewise bilinear interpolation of the coarse grid values.

### 4 Results

We first present the results for an undervolted gap filled with  $\text{N}_2$  at 300 K and at atmospheric pressure. A Gaussian initial condition has been taken for the electron and ion densities, with a maximum corresponding to  $10^{14}\text{ cm}^{-3}$  and a  $1/e$  radius of  $23\text{ }\mu\text{m}$ . The seed is situated on the axis of symmetry on the cathode, and a Neumann boundary condition is imposed at the cathode, allowing a net influx of electrons into the system. The distance between the electrodes is 15 cm, with a background electric field of 30 kV/cm. The boundary in the radial direction is put at a distance of 7.5 cm from the axis of symmetry. The grids are refined up to a size of  $4.6\text{ }\mu\text{m}$ . The transversal and longitudinal diffusion coefficients,  $D_L$  and  $D_T$ , are taken as  $D_L=1800\text{ cm}^2/\text{s}$  and  $D_T=2190\text{ cm}^2/\text{s}$ . Figure 1 shows the contourlines of the logarithm of the electron density, the net charge density and electric field strength at  $t=30, 60, 90$  and  $99\text{ ns}$ . The field plotted is the self-induced field of the streamer. The dotted lines represent a net positive charge, and a field lower than the background field. The beginning of the streamer propagation is the electron avalanche,

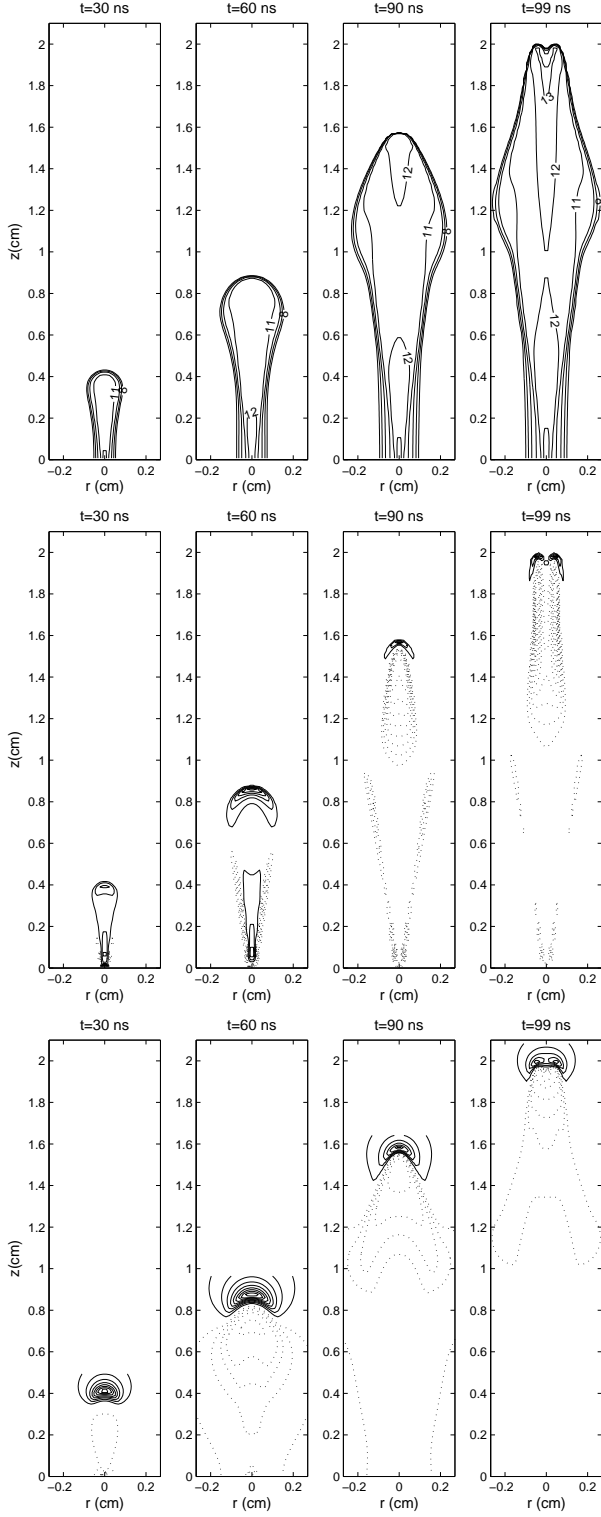


Figure 1: Contourlines of (starting from the upper figure)  $\log_{10} n_e$ , and in linear scale:  $n_+ - n_e$  and  $|\mathbf{E}| - E_0$ , at  $t=30, 60, 90$  and  $99$  ns. The initial ionization seed is a Gaussian with maximal value of  $1 \text{ cm}^{-3}$  and  $1/e$  radius of  $23 \mu\text{m}$ . The background field is of  $30 \text{ kV/cm}$ , pointing towards the cathode which is situated at  $z = 0$ . The dotted lines correspond to positive levellines in the middle figure, and to negative levellines in the lower figure.

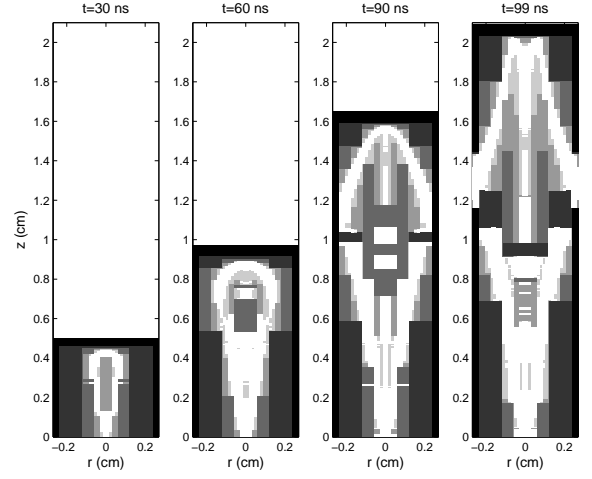


Figure 2: The computational grids at  $t=30, 60, 90$  and  $99$  ns. The gridcolor scales with the gridsize, the finest grids (with size  $4.6 \mu\text{m}$  in both directions) being white and the coarsest (with size  $147.2 \mu\text{m}$ ) being black.

characterized by a low space charge. In this phase, the electrons in the streamer head multiply and drift in the background field. The head behaves as the avalanche of an electron avalanche without inflow at the cathode: a Gaussian electron distribution propagating with a velocity  $E_0$ , undergoing diffusive widening. However, the total number of electrons in the avalanche is much larger than without inflow, which helps speeding up the build-up of space charge, and thereby the transition to a streamer. A layer of net space charge appears, grows thinner and becomes denser and denser, resulting in a strong field enhancement ahead of it. At  $t=99$  ns the streamer has gone off axis. From then the radial symmetric system has no realistic physical meaning anymore, and the simulations are stopped. Figure 2 shows the computational grids at the same times as the plots in Figure 1. The finest grids, with size  $4.6 \mu\text{m}$ , are drawn in white, the coarsest grid, with size  $147.2 \mu\text{m}$ , in black. Clearly the refinement criterion for the continuity grids selects the charged layer and the streamer base, where there are high gradients in the electron and net charge densities. A part of the streamer interior is shielded from the outer electric field, and the grids do not refine in that region. This comes from the fact that the low electric field induces a smaller spatial error in the discretization of the drift term.

In Figure 3 the different stages of the streamer propagation can be viewed. There the contours of the position  $z_m$  of the maximum of the net charge density is plotted as a function of the radial dis-

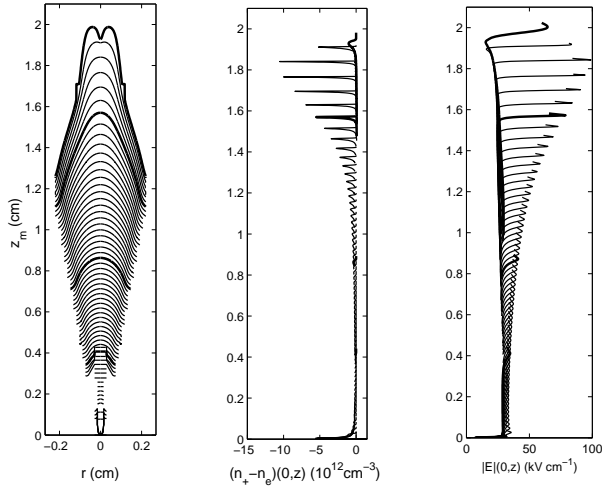


Figure 3: Left: contourlines of position  $z_m(r)$  of the maximal net charge density as a function of the distance from the  $r$ -axis for equidistant timesteps of 1.5 ns. Net charge density (middle) and electric field strength (right) along the  $r$ -axis for the same times. The thick lines correspond to  $t=30, 60, 90$  and  $99$  ns. The initial condition and background field are the same as in Fig. 1.

tance, at equidistant times ( $\Delta t=1.5$  ns). The second and third graphs in Figure 3 show, respectively, the net charge density and the electric field strength on the axis of symmetry at the same times. In both cases the values computed on the finest grid covering the streamer head are used. The thick lines correspond to the times of the snapshots in Figure 1. After some artifacts at very early times (at  $z < 0.1$  cm), the ionization front initially propagates uniformly in the constant external field, as an avalanche. Eventually, the curved space charge layer builds up, enhancing the field ahead of the streamer front. The streamer front therefore accelerates, but not uniformly because the streamer creates a spatial structure in the field. Indeed, the field is mostly enhanced near the axis of symmetry, in the tip of the streamer. That region therefore propagates faster than the “flank” of the streamerhead. This field enhancement is small up to  $t=60$  ns, so this effect is not yet visible. Then from  $t=60$  ns the field enhancement does become pronounced at the tip, resulting in an acceleration of the tip compared to the flank. The curvature of the front increases with time up to  $t=90$  ns. From that time, the tip itself accelerates even faster, whereas the flanks on the contrary decelerate. This is a result of the growing curvature of the front, which concentrates the field around the region where the curvature of the net charge density distribution is largest. The cur-

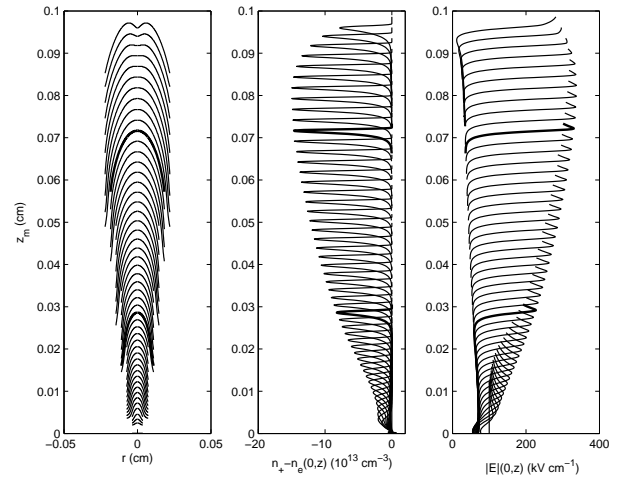


Figure 4: Left: contourlines of position  $z_m(r)$  of the maximal net charge density as a function of the distance from the  $r$ -axis for equidistant timesteps of 15 ps. Net charge density (middle) and field strength (right) along the  $r$ -axis for the same times. The same initial condition is used as in previous figures, but the background field is now set to 100 kV/cm. The thick lines correspond to  $t=0.3$  and  $0.6$  ns.

vature of the tip decreases, and the streamer tip approaches a planar streamer front. Such a planar front is known to be unstable [9], and indeed the streamer has branched at  $t=99$  ns.

The same initial seed in an overvolted gap with background field of 100 kV/cm shows a qualitatively comparable propagation. Because of the high background field the propagation is much more rapid than in the undervolted gap, and the branching state is reached in a similar manner but at a much earlier time (see Figure 4). The whole evolution towards splitting is a factor hundred fast compared to the low field case, while the velocities are roughly a factor four higher, and the whole distance covered by the streamer up to splitting is twenty times smaller.

## 5 Discussion and conclusions

The local uniform grid refinements allow us to simulate relatively large systems, much larger than would be possible on a uniform grid, within a reasonable computational time. In an undervolted gap, an electron avalanche eventually builds up enough space charge to create a field enhancement in the streamer head. The transition to streamer is accelerated by letting electrons flow into the system at the cathode. The tip of the streamer propagates more rapidly than the streamer flanks, concentrating and enhanc-



ing its own field, and finally reaching an unstable state. In an overvolted gap, the same initial seed also branches, though at a much earlier stage.

The final flattening of the streamer tip is not intuitive. A first hypothesis would be that the radial field component becomes large at the tip, tearing electrons away from the axis, thereby flattening the front. Another possibility would be that the field inside the streamer pushes the electrons away from the axis. These hypotheses still need some thorough investigation.

The implemented algorithm makes it possible to investigate, within a reasonable computational time, a wide variety of discharge conditions. It can be used for long systems with a low background electric field, and permits a high accuracy in the calculations for high fields, where the high streamer velocity gives rise to a steeper gradients and therefore larger numerical difficulties.

## References

- [1] F.F. Chen, Phys. Plasmas **2** (1995) 2164-2175
- [2] U. Kogelschatz, Plasma Source Sc. and Tech. **11** (2002) 29-36
- [3] V.P. Pasko and H.C. Stenbaek-Nielsen, Geophys. Res. Letters **29** (2002) 82/1-4
- [4] Y.P. Raizer, *Gas discharge physics*, Springer-Verlag, Berlin (1997), p.56
- [5] S.K. Dhali and P.F. Williams, J. Appl. Phys **2** (1987) 4696-4706
- [6] P.A. Vitello, B.M. Penetrante and J.N. Bardsley, Phys. Rev. E **49** (1994) 5574-5598
- [7] R.A. Trompert and J.G. Verwer, Appl. Num. Math. **8** (1991) 65-90
- [8] W. Hundsdorfer and J.G. Verwer, *Numerical solution of time-dependent advection-diffusion-reaction equations*, Springer, Berlin (2003) p.217
- [9] M. Arrayás and U. Ebert, Phys. Rev. E **69** (2004) 036214/1-10